

ANALYSIS OF PERFORMANCE FLUCTUATIONS FOR THE CERN PROTON SYNCHROTRON MULTI-TURN EXTRACTION

A. Huschauer*, M. Giovannozzi, O. Michels, A. Nicoletti, G. Sterbini, CERN, Geneva, Switzerland

Abstract

After the successful beam commissioning and tests in 2015, the Multi-Turn Extraction (MTE) has been put in operation in 2016. In this paper, the remaining issues related with fluctuation of the MTE performance are evaluated and correlation studies are presented in view of estimating the impact of planned improvements.

INTRODUCTION

To provide high-intensity beams for fixed-target physics at the Super Proton Synchrotron (SPS), the beam delivered by the PS has to be fully de-bunched and uniform in intensity. Therefore, the Continuous Transfer (CT) process was proposed in 1973 [1]. This extraction technique, which occurs over five turns at 14 GeV/c, allows to optimize the duty cycle as only two subsequent extractions from the PS are necessary to fill the SPS. On the downside, the CT extraction comes with the major drawback of significant beam loss occurring at multiple locations around the ring [2], leading to high dose to personnel during accelerator maintenance and repair, as well as to long cool down times.

The Multi-Turn Extraction (MTE) technique was proposed to replace the CT process in 2001 [3] in view of mitigating the shortcomings of CT. MTE is a resonant extraction mechanism, which exploits advanced concepts of non-linear beam dynamics and applies a fourth-order stable resonance to perform beam splitting in the horizontal phase space. The resulting beamlets - four islands and one core - are then extracted over five subsequent turns (see [4] for the implementation and [5] for some theory of adiabatic trapping).

Due to the complexity of the MTE scheme, its operational implementation, which came to a successful close in September 2015 (see [6, 7] for more detail), has had to overcome many challenges and, particularly, significant fluctuations in the efficiency of the transverse splitting, defined as

$$\eta_{MTE} = \frac{\langle I_{\text{Island}} \rangle}{I_{\text{Total}}}, \quad (1)$$

where $\langle I_{\text{Island}} \rangle$ and I_{Total} stand for the average intensity in each island and the total beam intensity, respectively. The nominal efficiency is 0.20, corresponding to an equal beam sharing between islands and core. This figure of merit is derived from the signal of the beam intensity in the transfer line, just downstream of the PS extraction point.

Figure 1 shows the distribution of η_{MTE} during the 2016 physics run. The shape is quasi-Gaussian, skewed towards low values of η_{MTE} . Understanding the fine detail of this distribution and finding means to improve it, i.e., reducing

its spread, are the goal of the studies discussed in this paper.

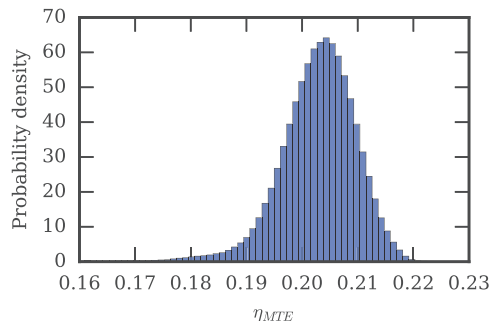


Figure 1: Distribution of η_{MTE} for the 2016 physics run.

ANALYSIS OF FLUCTUATIONS

Figure 2 (left) shows the time-evolution of η_{MTE} over five days. In addition to the raw data, the time series sampled over non-overlapping time intervals of 30 min is shown as well. The comparison of these signals reveals low- and high-frequency structures.

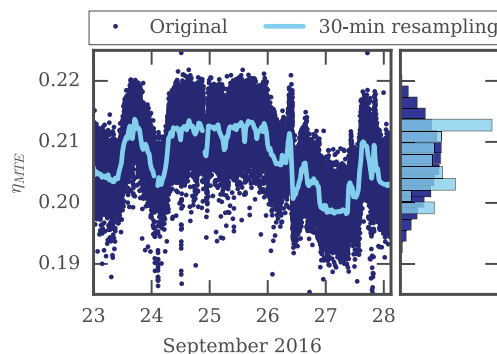


Figure 2: Time evolution of η_{MTE} and of its re-sampled version over non-overlapping intervals of 30 min (left) and their distributions (right).

The corresponding distributions are shown in Fig. 2 (right). While the distribution of the raw data is quasi-Gaussian, this is by far not the case for the low-frequency contribution. These features suggest a different physical source and, therefore, different mitigation strategies to the fluctuations of η_{MTE} . In fact, the low-frequency variations can be cured by a slow feedback or by a human intervention, while the high-frequency components cannot. Therefore, most of the efforts have been devoted to finding the sources of the high-frequency variation in view of correcting them at the source.

An example of the time-variations that can be corrected by a human intervention is given in Fig. 3 (upper), where a slow drift of the PS transverse tunes is shown together

* alexander.huschauer@cern.ch

with the change in η_{MTE} (lower). Even though the origin

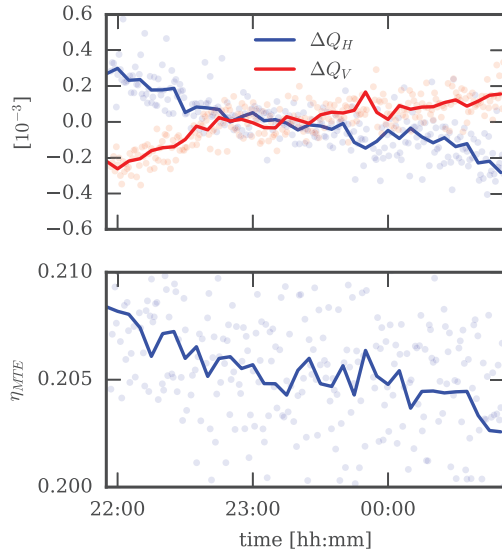


Figure 3: Upper: Time evolution of ΔQ_H and ΔQ_V . Lower: Time evolution of η_{MTE} . The continuous lines represent the re-sampled version over non-overlapping intervals of 5 min.

of the tune drift is not known, the time scale is such that the variation can be compensated by means of the PS ring tuning quadrupoles. Another example is given by the impact of the change of the PS magnetic configuration on η_{MTE} , shown in Fig. 4. A step variation is clearly visible, which is likely to be generated by a change in the hysteresis of the combined-function main magnets. Also in this case the change in η_{MTE} can be easily compensated by acting on the horizontal tune.

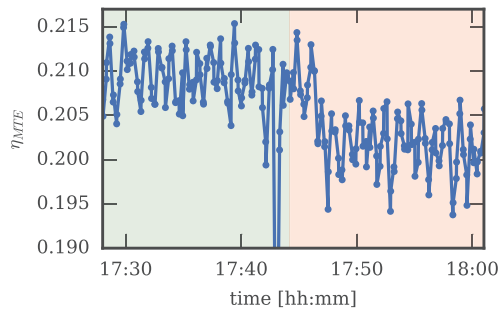


Figure 4: Time evolution of η_{MTE} during a change of PS magnetic configuration (indicated by the change of colour of the background).

CORRELATION ANALYSIS

The main source of the high-frequency fluctuations was identified as the 5 kHz ripple component of the converters powering the additional coils installed in the main magnets [6]. The clocks of these six power converters are not synchronised, thus generating a time-dependent ripple component. The excellent correlation between the amplitude variation of this ripple component and η_{MTE} is shown in Fig. 5 (upper). The measurement device installed in a reference magnet provides the value of dB/dt .

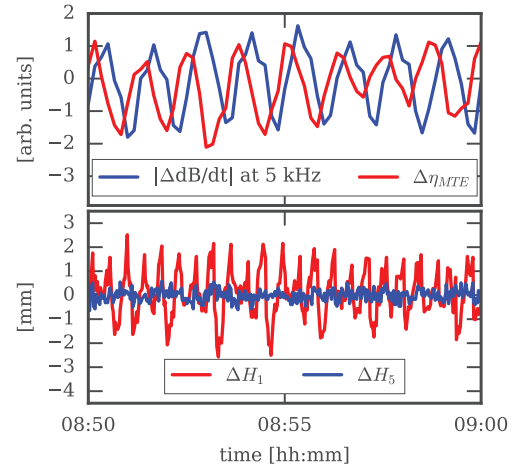


Figure 5: Upper: Time evolution of η_{MTE} and of the amplitude of the 5 kHz current ripple component on the power supplies. Lower: Time evolution of the variation of extraction conditions of first island (ΔH_1) and of core (ΔH_5).

Hence, the observed $\pi/2$ phase difference between η_{MTE} and dB/dt turns into a π phase difference with the B -field, which then is in counter phase with η_{MTE} . All this is a sign of the good correlation between the two quantities, not to mention that the two quantities feature a very similar time variation. It is also interesting to inspect the behaviour of the horizontal extraction position as a function of time. To analyse the trajectory stability of the extracted beam, a pick-up in the transfer line just downstream of the PS extraction septum is used to determine the position of each extracted turn. The average position over several extractions is subtracted from the measured value and the result is indicated by ΔH_i , $1 \leq i \leq 5$. The analysis showed that ΔH_i , $1 \leq i \leq 4$ are all well correlated between them, as expected, so that it is sufficient to consider in the analysis only ΔH_1 and ΔH_5 , i.e., the horizontal variation of the extraction condition of the first island and of the core, respectively. Their time evolution is shown in Fig. 5 (lower): while ΔH_5 is almost constant, with a variation close to the pick-up resolution, ΔH_1 changes considerably. Furthermore, the frequency content appears different with respect to the 5 kHz ripple component. This behaviour, however, does not imply that the fluctuations of ΔH_1 are not related with the ripple. In fact, the ripple affects η_{MTE} during the resonance crossing stage extending over several tens of ms, so that its phase is irrelevant. On the other hand, the extraction conditions are indeed sensitive not only to the amplitude, but also to the phase of the 5 kHz component with respect to the extraction time.

This analysis can be further pursued by checking the autocorrelation of η_{MTE} and ΔH_1 , as shown in Fig. 6. The former quantity features a rather regular pattern, showing that a strong correlation (positive or negative) occurs for time intervals slightly over one minute, while ΔH_1 features a slightly weaker autocorrelation, much richer in frequency content. The striking point is the close resemblance of the autocorrelation of η_{MTE} and ΔH_1 with that of the amplitude and phase of the 5 kHz component, respectively. All this is

clearly visible in Fig. 6, thus confirming that the ripple is the source of both η_{MTE} fluctuations and ΔH_1 variations.

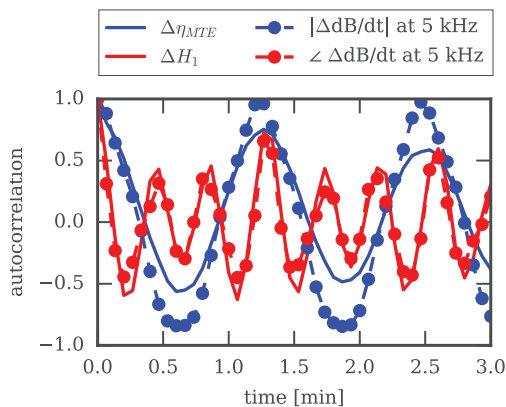


Figure 6: Autocorrelation of η_{MTE} (blue) and ΔH_1 (red).

From an operational point of view, given that two extractions from the PS are needed to fill the SPS ring, the performance of consecutive extractions should be very similar. This turns out to be the case as can be seen in Fig. 7, where the correlation between the two extractions for η_{MTE} and ΔH_1 is clearly visible.

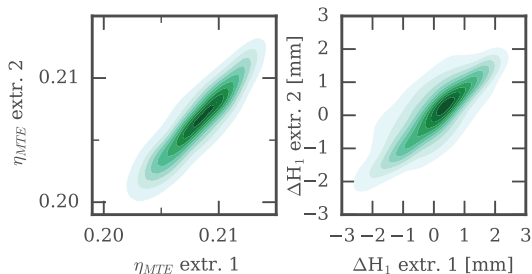


Figure 7: Correlation plot of two consecutive extractions for η_{MTE} (left) and for ΔH_1 (right). The correlation coefficients for η_{MTE} and ΔH_1 are 0.84 and 0.74, respectively.

The last aspect analysed is the correlation between fluctuations and extraction losses. To this aim, the signal from a beam loss monitors (BLM) installed close to the extraction septum (SS16) has been used (see also [6, 8]). The BLM detects two loss spikes generated by the continuous beam during the rise time of the extraction kickers, when the islands and then the core are extracted. These two spikes are individually integrated and correlated with η_{MTE} in Fig. 8. The best correlation between η_{MTE} and beam losses is observed for the core. The observation that the core-induced beam losses are closely connected with the fluctuations of η_{MTE} is confirmed by the result that the core width is well correlated with η_{MTE} as shown in Fig. 9. The core width can be estimated by means of a diamond BLM also installed in SS16. In fact, the time-response of a diamond BLM is fast enough to ensure that the FWHM of the loss spike is proportional to the beam width.

The results shown in Fig. 9 indicate that a smaller core size implies a larger η_{MTE} and hence lower losses at extraction.

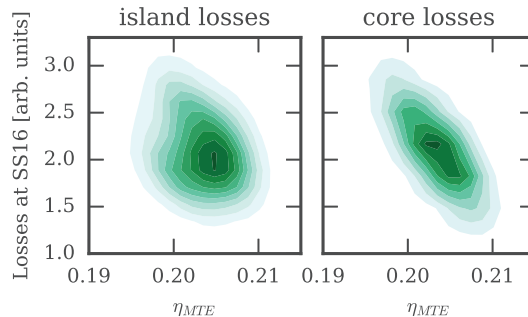


Figure 8: Correlation plot of losses for islands (left) and core (right) and η_{MTE} . The correlation coefficients for islands and core losses are -0.19 and -0.75 , respectively.

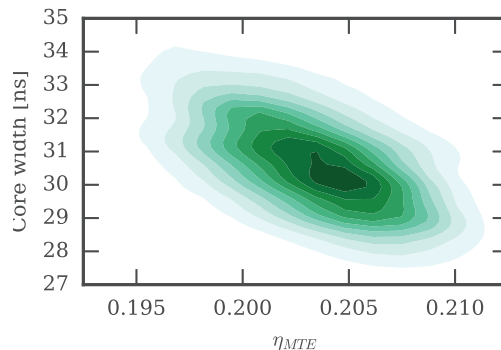


Figure 9: Correlation between core size and η_{MTE} . The correlation coefficient is -0.54 .

CONCLUSIONS AND OUTLOOK

The efforts devoted to the understanding of the fluctuations of η_{MTE} are paying off. The mitigation measures put in place in 2015 to reduce the amplitude of the 5 kHz ripple of the power converters of the auxiliary coils in the PS main magnets made MTE a suitable operational replacement of CT. The measurements and analysis presented in this paper confirm that η_{MTE} correlates well with the power converter ripple. For this reason the controls of the power converters have been upgraded during the 2016-17 winter shut down so to allow synchronising the clocks and to double the ripple frequency, thus shifting it outside of the beam spectrum [8]. New current transformers have been installed to provide a direct current measurement for the auxiliary circuits and should provide additional information to assess which field component affects η_{MTE} and ΔH_1 . The new observations presented here indicate that curing the ripple should have a beneficial impact on the reproducibility of the extraction trajectories and should lower extraction losses, whose fluctuations are linked with the beam core size. Finally, after the successful reduction of the high-frequency η_{MTE} fluctuations, only the low-frequency components will remain.

ACKNOWLEDGEMENT

Our warm thanks go to the PS Operations crew, and to G. Arduini, J.-P. Burnet, K. Kahle, M. Martino, R. Steerenberg for continuous support, encouragement and help.

REFERENCES

- [1] C. Bovet, D. Fiander, L. Henny, A. Krusche, and G. Plass, “The fast shaving ejection for beam transfer from the CPS to the CERN 300 GeV machine”, *IEEE Trans. Nucl. Sci.* **20**, 438 (1973).
- [2] J. Barranco García and S. Gilardoni, “Simulation and optimization of beam losses during continuous transfer extraction at the CERN Proton Synchrotron”, *Phys. Rev. ST Accel. Beams* **14**, 030101 (2011).
- [3] R. Capi and M. Giovannozzi, “Novel method for multiturn extraction: trapping charged particles in islands of phase space”, *Phys. Rev. Lett.* **88**, 104801 (2002).
- [4] M. J. Barnes, O. E. Berrig, A. Beuret, J. Borburgh, P. Bourquin, R. Brown, J.-P. Burnet, F. Caspers, J.-M. Cravero, T. Dobers, T. Fowler, S. Gilardoni, M. Giovannozzi (ed.), M. Hourican, W. Kalbreier, T. Kroyer, F. Di Maio, M. Martini, V. Mertens, E. Métral, K.-D. Metzmacher, C. Rossi, J.-P. Royer, L. Sermeus, R. Steerenberg, G. Villiger, T. Zickler, “The CERN PS multi-turn extraction based on beam splitting in stable islands of transverse phase space: Design Report”, CERN-2006-011 (2006).
- [5] A. Bazzani, C. Frye, M. Giovannozzi, and C. Hernalsteens, “Analysis of adiabatic trapping for quasi-integrable area-preserving maps”, *Phys. Rev. E* **89**, 042915 (2014).
- [6] J. Borburgh, S. Damjanovic, S. Gilardoni, M. Giovannozzi, C. Hernalsteens, M. Hourican, A. Huschauer, K. Kahle, G. Le Godec, O. Michels, and G. Sterbini, “First implementation of transversely split proton beams in the CERN Proton Synchrotron for the fixed-target physics programme”, *EPL* **113**, 34001 (2016).
- [7] S. Abernethy, A. Akroh, H. Bartosik, A. Blas, T. Bohl, S. Cettour-Cave, K. Cornelis, H. Damerau, S. Gilardoni, M. Giovannozzi, C. Hernalsteens, A. Huschauer, V. Kain, D. Manglunki, G. Métral, B. Mikulec, B. Salvant, J.-L. Sanchez Alvarez, R. Steerenberg, G. Sterbini, and Y. Wu, “Operational performance of the CERN injector complex with transversely split beams”, *Phys. Rev. Accel. Beams* **20**, 014001 (2017).
- [8] A. Huschauer, A. Blas, J. Borburgh, S. Damjanovic, S. Gilardoni, M. Giovannozzi, M. Hourican, K. Kahle, G. Le Godec, O. Michels, G. Sterbini, and C. Hernalsteens, “Transverse beam splitting made operational: key features of the multi-turn extraction at the CERN Proton Synchrotron”, submitted for publication.